Applied and Environmental Microbiology

# Inactivation of $Ca^{2+}/H^{+}$ Exchanger in Synechocystis sp. Strain PCC 6803 Promotes Cyanobacterial Calcification by Upregulating $CO_2$-Concentrating Mechanisms

**Hai-Bo Jiang, Hui-Min Cheng, Kun-Shan Gao and Bao-Sheng Qiu**

***Appl. Environ. Microbiol.*** **2013, 79(13):4048. DOI: 10.1128/AEM.00681-13.**
**Published Ahead of Print 26 April 2013.**

AEM
Journals.ASM.org

# Inactivation of $Ca^{2+}/H^{+}$ Exchanger in *Synechocystis* sp. Strain PCC 6803 Promotes Cyanobacterial Calcification by Upregulating $CO_2$-Concentrating Mechanisms

**Hai-Bo Jiang,[a] Hui-Min Cheng,[a] Kun-Shan Gao,[b] Bao-Sheng Qiu[a]**

College of Life Sciences, and Hubei Key Laboratory of Genetic Regulation and Integrative Biology, Central China Normal University, Wuhan, Hubei, People's Republic of China[a]; State Key Laboratory of Marine Environmental Science, Xiamen University, Xiamen, Fujian, People's Republic of China[b]

**Cyanobacteria are important players in the global carbon cycle, accounting for approximately 25% of global $CO_2$ fixation. Their $CO_2$-concentrating mechanisms (CCMs) are thought to play a key role in cyanobacterial calcification, but the mechanisms are not completely understood. In *Synechocystis* sp. strain PCC 6803, a single $Ca^{2+}/H^{+}$ exchanger (Slr1336) controls the $Ca^{2+}/H^{+}$ exchange reaction. We knocked out the exchanger and investigated the effects on cyanobacterial calcification and CCMs. Inactivation of *slr1336* significantly increased the calcification rate and decreased the zeta potential, indicating a relatively stronger $Ca^{2+}$-binding ability. Some genes encoding CCM-related components showed increased expression levels, including the *cmpA* gene, which encodes the $Ca^{2+}$-dependent $HCO_3^-$ transporter BCT1. The transcript level of *cmpA* in the mutant was 30 times that in wild type. A Western blot analysis further confirmed that protein levels of CmpA were higher in the mutant than the wild type. Measurements of inorganic carbon fluxes and $O_2$ evolution proved that both the net $HCO_3^-$ uptake rate and the BCT1 transporter supported photosynthetic rate in the *slr1336* mutant were significantly higher than in the wild type. This would cause the mutant cells to liberate more $OH^-$ ions out of the cell and stimulate $CaCO_3$ precipitation in the microenvironment. We conclude that the mutation of the $Ca^{2+}/H^{+}$ exchanger in *Synechocystis* promoted the cyanobacterial calcification process by upregulating CCMs, especially the BCT1 $HCO_3^-$ transporter. These results shed new light on the mechanism by which CCM-facilitated photosynthesis promotes cyanobacterial calcification.**

Cyanobacterial calcification occurs in lakes, springs, oceans, and terrestrial ecosystems and is involved in the fundamental process of the global carbon cycle (1–4). This process makes an important contribution to the formation of carbonate deposits, which are now intensively studied as high-resolution continental archives for environmental change (1, 5–8). Despite the recent finding of intracellular calcification in the cyanobacterium "*Candidatus* Gloeomargarita lithophora" (9), cyanobacterial calcification is usually an extracellular bio-induced process that is mediated by both environmental factors and biological processes. Although many of the genes and proteins involved in the cyanobacterial calcification process are yet to be elucidated, the following factors are assumed to be crucial: (i) calcium concentration (1); (ii) carbonate saturation state and availability of dissolved inorganic carbon (DIC) (8, 10); (iii) growth medium pH (11); (iv) temperature (12); (v) availability of nucleation sites, such as an exopolysaccharide sheath or a proteinaceous surface layer around the cells (13). Thus, examination of genes involved in $Ca^{2+}$, $H^{+}$, and DIC transport in cyanobacteria may help to elucidate the molecular mechanism of bio-induced extracellular calcification.

$CO_2$-concentrating mechanisms function to transport and actively accumulate DIC to elevate the $CO_2$ concentration around Rubisco (14–16). The constitutive forms of CCMs are obligate for cyanobacterial growth in most natural aquatic environments, while the inducible forms of CCMs are upregulated under DIC-limited conditions (16). In cyanobacterial cells, the active uptake of $CO_2$ or $HCO_3^-$ could lead to the release of equal amounts of $OH^-$ ions, which would increase the pH of the microenvironment around the cells. An increase in pH causes a shift in the carbonic acid equilibrium toward $CO_3^{2-}$, followed by $CaCO_3$ precipitation (3, 7, 8, 10, 17).

It remains controversial whether CCM-facilitated photosynthesis promotes the cyanobacterial calcification process, although several models of calcification mechanisms have proposed roles for photosynthesis and CCMs (3, 4, 10). Merz (10) reported that the calcification in mats of the filamentous cyanobacteria *Schizothrix* sp. and *Scytonema* sp. decreased upon addition of ethoxyzolamide (EZ; a membrane-permeable carbonic anhydrase inhibitor) or DCMU [3-(3,4-dichlorophenyl)-1,1-dimethylurea], a PSII electron transport inhibitor. These findings suggested that $CaCO_3$ precipitation is quantitatively related to photosynthesis and CCMs. Geological records also suggest that cyanobacterial calcification is promoted by CCMs (3, 17). The atmospheric $CO_2$ partial pressure has been estimated to fall below approximately 0.4% around the Devonian-Mississippian transition (ca. 360 million years), a level currently sufficient to induce CCMs in cyanobacteria. Meanwhile, microfossil records indicate that sheath-calcified cyanobacteria (*Girvanella*) appeared during the Mississippian, ca. 325 to 355 million years, which coincides with the development of CCMs (3, 17). However, Obst et al. (18) found that photosynthesis did not directly influence the nucleation process of $CaCO_3$ on the

**Received** 5 March 2013 **Accepted** 19 April 2013
**Published ahead of print** 26 April 2013
Address correspondence to Bao-Sheng Qiu, bsqiu@mail.ccnu.edu.cn.
H.-B.J. and H.-M.C. contributed equally to this work.
Supplemental material for this article may be found at http://dx.doi.org/10.1128/AEM.00681-13.

doi:10.1128/AEM.00681-13

cell surface of *Synechococcus leopoliensis* PCC 7942 under low-nutrient concentrations and continuous $CO_2$ supply. A DCMU or dark treatment had little effect on precipitation rates (18). Thus, more studies are required to clarify the relationship between cyanobacterial calcification and CCM-facilitated photosynthesis.

The freshwater unicellular cyanobacterium *Synechocystis* sp. strain PCC 6803 (here *Synechocystis* 6803) is an important model species for CCM research (14–16). This strain was the first phototrophic organism to be fully sequenced, and it is amenable to genetic manipulation. In *Synechocystis* 6803, Slr1336 (named SynCAX) has been identified as the only $Ca^{2+}/H^+$ exchanger. This protein is located in the plasma membrane and catalyzes the $Ca^{2+}/H^+$ exchange reaction at alkaline pH with a stoichiometry of $H^+$:$Ca^{2+}$ that is higher than 2 (19). The characteristics of the SynCAX protein, which transports $Ca^{2+}$ out and $H^+$ into the cells, make it an ideal candidate to investigate cyanobacterial calcification. In this study, we conducted a comparative analysis of *Synechocystis* 6803 wild type and a $Ca^{2+}/H^+$ exchanger mutant (*slr1336*::C.K2) to investigate the molecular mechanism of cyanobacterial calcification and its relationship with CCM-facilitated photosynthesis.

## MATERIALS AND METHODS

**Strains and culture conditions.** A glucose-tolerant wild-type strain of *Synechocystis* 6803 was cultured in BG11 liquid medium (20) supplemented with 3.4 mM $CaCl_2$ and 1 mM $KHCO_3$ at 30°C under continuous fluorescent cool white lights (40 μmol photons $m^{-2}$ $s^{-1}$). According to the culture requirements of the mutants or complemented strains, kanamycin (25 μg $ml^{-1}$), spectinomycin (20 μg $ml^{-1}$), or both were added to the BG11 medium. All samples were cultured under these photoautotrophic growth conditions unless stated otherwise. For light-activated heterotrophic growth, 5 mM glucose was added to the culture medium. Samples were exposed to 40 μmol photons $m^{-2}$ $s^{-1}$ light for 5 min per day but otherwise kept in the dark (21). Growth was monitored by cell counting with an Epics Altra flow cytometer (Beckman Coulter, Cupertino, CA), with a known concentration of yellow-green fluorescent microspheres (1.00-μm-diameter beads, catalog number 18860; Polysciences Inc., Warrington, PA) (22). Specific growth rates were calculated as the slopes of the linear regression of the ln(cell concentration) versus day for individual cultures over the linear range.

**Plasmid construction and generation of cyanobacterial mutants and the complemented strain.** Molecular manipulations were performed using standard methods. Enzymes were used according to the manufacturers' instructions. The primers used for PCR amplifications are listed in Table S1 in the supplemental material.

Plasmids for gene disruption were constructed as follows: DNA fragments containing the *slr1336* gene or the *cmpA* (*slr0040*) gene were amplified from the genomic DNA of *Synechocystis* 6803 by using the primers slr1336-F/slr1336-R or CmpA-1/CmpA-2, respectively. The obtained sequences were cloned into pMD18-T (TaKaRa) and confirmed by sequencing. The C.K2 (kanamycin resistance) cassette was inserted into the NcoI site of the plasmid pMD18-T::*slr1336*, resulting in plasmids pHS062 for the inactivation of *slr1336* in *Synechocystis* 6803. Similarly, the *omega* cassette was inserted into the ClaI site of the plasmid pMD18-T::*slr0040*, resulting in plasmid pHS462 for the inactivation of *cmpA* in *Synechocystis* 6803.

The plasmid for complementation was constructed as follows: the *slr1336* gene fragment was amplified from the genomic DNA of *Synechocystis* 6803 by using the primers slr1336c-F and slr1336c-R and *Pfu* DNA polymerase (Promega). The PCR fragment was confirmed by sequencing and then cloned into the NdeI site of the PpsbAII expression platform (pHS298) (23).

Transformation of *Synechocystis* 6803 was performed as described by Williams (24). The mutants and complemented strain were generated by transformation with the corresponding plasmids. Complete segregation of mutants was confirmed by PCR.

**Calcium precipitation experiments.** Calcium precipitation experiments were performed at pH 8.0 under photoautotrophic and light-activated heterotrophic growth conditions and with 20 mM HEPES-KOH buffer. The amount of $CaCO_3$ precipitated per time interval per cell was determined after 3 h. Cell numbers at the beginning and the end of experiments were determined by flow cytometry. The precipitated calcium was presumed to be absent from the filtered supernatant solution. At the end of the experiments, samples were centrifuged, and the supernatants were filtered through a 0.22-μm nylon filter and then acidified with $HNO_3$. The concentration of calcium precipitated in each vial was calculated by subtracting the concentration of calcium in the supernatant from the original amount of calcium added. All filtered solutions were analyzed to determine the aqueous $Ca^{2+}$ concentration by atomic absorption spectroscopy (Varian spectrophotometer AA240 FS), and 2% $SrCl_2$ was added before analysis (25).

**Electrophoretic mobility assay.** The electrophoretic mobilities of cell suspensions were measured using a Zetasizer Nano ZS90 instrument (ZEN3690; Malvern Instruments Ltd., United Kingdom). The zeta potential was calculated from the measured mobility according to the Smoluchowski equation, and samples were prepared as described by Dittrich and Sibler (26).

**Measurement of intracellular pH.** For cell dying, 5(6)-carboxyfluorescein diacetate (CF-DA; Sigma) was dissolved in dimethyl sulfoxide (DMSO) to a final concentration of 10 mM. For calibration, the deesterified probe 5(6)-carboxyfluorescein (CF; Sigma) was dissolved in DMSO to a final concentration of 100 mM. These solutions were diluted with BG11 medium buffered with 20 mM HEPES-KOH (pH 8.0) or 20 mM CAPS-KOH (pH 10.0) to obtain 10 μM CF-DA or 40 μM CF, respectively. For calibration purposes, we prepared 50 mM citric disodium hydrogen phosphate buffers from pH 4.96 to 7.41 in steps of 0.20 pH units. Cells at exponential phase were harvested, washed, and resuspended in pH 8.0 or pH 10.0 BG11 medium for 3 h at 40 μmol photons $m^{-2}$ $s^{-1}$ and 30°C. Then, these cells were incubated with the pH probe solution for 30 min in the dark at 37°C. For *in vivo* calibration, 13 μM nigericin (Sigma) was added to the samples to equilibrate the pH of stained cells to the pH of the surrounding buffer. Analysis of the fluorescence intensity of individual cells was performed using an Epics Altra flow cytometer (Beckman Coulter). Samples were excited with a 488-nm argon ion laser, while the fluorescence emission was measured through 525-nm and 575-nm bandpass filters (27). All data were acquired in logarithmic mode with a total of 20,000 cells measured for every sample.

**Quantitative reverse transcription-PCR (qRT-PCR).** Cells were collected by a brief centrifugation (4,800 × *g*, 6 min), and total RNA was isolated with a TRIzol reagent kit (Invitrogen). To remove DNA contamination, the RNA solutions were digested with 4 U RNase-free DNase (Promega) according to the manufacturer's instructions. The digest was extracted with an equal volume of phenol-chloroform-isoamyl alcohol (25:24:1), and the RNA was precipitated by centrifugation after overnight incubation at −80°C in the presence of 200 mM LiCl and 75% (vol/vol) ethanol.

For quantitative RT-PCR analysis, first-strand synthesis was carried out using Moloney murine leukemia virus reverse transcriptase (Promega) according to the manufacturer's instructions. For PCR amplifications, we used the cDNA products and primers specific for the following CCM-related genes: *cmpA*, *bicA*, *sbtA*, *ndhF3*, *ccaA*, *ecaB*, and *ccmN*. The RNase P subunit B gene (*rnpB*) served as the control. Amplifications were carried out in a 20-μl volume using SYBR green real-time PCR master mix (Toyobo). The primers used in these experiments are provided in Table S1 of the supplemental material. Relative quantification of transcripts in this study was carried out using the following $2^{-\Delta\Delta CT}$ method, described by Livak and Schmittgen (28): $\Delta\Delta C_T = (C_{T,\,\text{Target}} - C_{T,\,rnpB})_{slr1336\ \text{mutant}} - (C_{T,\,\text{Target}} - C_{T,\,rnpB})_{\text{wild type}}$.

**Western blot analysis.** For Western blot analysis, cells were collected by centrifugation, resuspended in 40 mM Tris-HCl (pH 8.0) with 1 mM phenylmethylsulfonyl fluoride (PMSF), and ruptured with a UP200S ultrasonic processor (Hielscher Ultrasound Technology, Germany) in an ice bath for 15 min at 40% amplitude and 0.3 cycles. Cell debris and unbroken cells were removed by centrifugation at 11,000 × *g* at 4°C for 10 min. The supernatant was used for the Western blot analysis. SDS-PAGE and Western blotting were performed using standard methods. Equal amounts of proteins were loaded, separated by 12% SDS-PAGE, transferred to nitrocellulose filters (Millipore, Ireland), detected with anti-CmpA rabbit antiserum (which was obtained from rabbits immunized with purified CmpA), and visualized with goat anti-rabbit alkaline phosphatase antibody with nitroblue tetrazolium (NBT) and 5-bromo-4-chloro-3- indolylphosphate (BCIP; Amresco) as the substrates.

**CA activity assays.** The carbonic anhydrase (CA) assay was based on the rate of change in pH value after the injection of a standard amount of $CO_2$-saturated water (29). Samples were collected by centrifugation, resuspended in pH 8.0 assay buffer (40 mM HEPES, 40 mM $MgCl_2$, and 4 mM PMSF), and ruptured by ultrasonication in an ice bath. Then, 5 ml of supernatant was added to a stirred, water-jacketed cuvette (4°C), with a pH electrode inserted into the assay solution. After the temperature equilibrated, 5 ml ice-cold $CO_2$-saturated water was injected, and the time for the pH to change from 8.0 to 7.0 was recorded. The buffer without cell crude extract was used as the control. CA activity was calculated as the difference in the initial rate of $CO_2$ hydration between the control and the samples and is expressed in Wilbur-Anderson units (WAU) per 1 mg of protein. One WAU is defined as $10 \times (t_0 - t)/t$, where $t_0$ and $t$ are the times (in minutes) required for the pH to change by ΔpH in the control and the sample, respectively.

**$C_i$ flux measurements with MIMS.** For inorganic carbon ($C_i$) flux measurements with a membrane inlet mass spectrometer (MIMS), cells were harvested by brief centrifugation and then resuspended in fresh modified BG11 medium (no $Na_2CO_3$, and $NaNO_3$ was replaced with an equal amount of KCl, supplemented with 25 mM NaCl, and buffered with 20 mM HEPES-KOH at pH 8.0) as described by Song and Qiu (30). The $CO_2$ ($m/z = 44$) and $O_2$ ($m/z = 32$) concentrations in the cell suspensions were monitored simultaneously by using a thermostat-controlled glass cuvette connected to a membrane inlet mass spectrometer (HPR40; Hiden). The dark/light/dark intervals lasted about 6 min at 30°C. During dark intervals, 100 μM $KHCO_3$ was added before the beginning of the subsequent light interval (light intensity, 500 μmol photons $m^{-2}$ $s^{-1}$). Net $HCO_3^-$ uptake, net $CO_2$ uptake, leakage of $CO_2$, and influx of $CO_2$ were estimated according to the methods described by Badger et al. (31). The rate constants for the conversion of $HCO_3^-$ to $CO_2$ were 0.0508 $s^{-1}$ for $k_1$ ($CO_2 \rightarrow HCO_3^-$) and 0.00087 $s^{-1}$ for $k_2$ ($HCO_3^- \rightarrow CO_2$). Before $C_i$ flux measurements, MIMS was calibrated for $O_2$ concentrations with air-equilibrated and oxygen-free distilled water. MIMS was calibrated for $CO_2$ concentrations by injecting known amounts of $NaHCO_3$ into 0.2 mM HCl and adding known amounts of NaOH into $C_i$-free distilled water.

**Measurements of photosynthetic activities of cells.** SbtA and BicA $HCO_3^-$ transporters depend on millimolar levels of $Na^+$ and are specifically inhibited by $Li^+$ ions, which have little effect on other modes of $C_i$ uptake (32, 33). EZ is a membrane-permeable CA inhibitor that specifically inhibits active $CO_2$ uptake (34). To determine the contribution of different $C_i$ transporters to photosynthesis, samples were collected, washed, and resuspended in $NO_3^-$, $Na^+$, and $C_i$-free BG11 medium buffered with 20 mM HEPES-KOH (pH 8.0) as described previously (30), and then 2-ml aliquots of cell suspensions were placed into an oxygen electrode chamber (Chlorolab 2; Hansatech Instruments Ltd., King's Lynn, Norfolk, United Kingdom). After DIC depletion at 150 μmol photons $m^{-2}$ $s^{-1}$ for about 30 min, photosynthetic activities were measured as oxygen evolution under the three treatments (25 mM NaCl, 25 mM NaCl plus 300 μM EZ, or 25 mM LiCl plus 300 μM EZ) at 650 μmol photons $m^{-2}$ $s^{-1}$ and 30°C with supplementation of 1 mM $KHCO_3$.

## RESULTS

**Growth and pH changes.** To obtain the $Ca^{2+}/H^+$ exchanger mutant in *Synechocystis* 6803, a kanamycin resistance cassette was inserted into the NcoI site of the *slr1336* gene in the *Synechocystis* genome. The complete segregation mutant was obtained by growing cells for many generations on kanamycin-containing medium and was confirmed by PCR (see Fig. S1 in the supplemental material). When cultured under photoautotrophic conditions, the *slr1336*::C.K2 mutant showed a slightly lower growth rate (0.83 ± 0.01) than that of the wild type (0.89 ± 0.01 [mean ± standard deviation, or SD, of slopes of the linear regression of the ln of the cell concentration versus day for individual cultures over the linear range]) (*t* test, $P < 0.05$) (Fig. 1A). In cultures of the wild type and *slr1336*::C.K2, the pH of the growth medium increased from 8.0 to approximately 10.34 and 10.54, respectively, after the first 4 days and then decreased to approximately 9.20 and 9.07, respectively (Fig. 1A). However, under light-activated heterotrophic growth conditions, there were no significant differences in either the specific growth rate or growth medium pH between the two strains (Fig. 1B). The slight growth delay of the *slr1336*::C.K2 mutant under photoautotrophic conditions was probably because of a change in intracellular pH. Results showed that when the outside medium pH was 8.0, the intracellular pH was not significantly different between the wild-type and mutant cells (*t* test, $P > 0.05$), but when the medium pH was 10.0, the intracellular pH of *slr1336*::C.K2 was significantly higher than that of the wild type (*t* test, $P < 0.05$) (Fig. 1D). Under photoautotrophic growth conditions, cells conducted photosynthesis and assimilated $CO_2$ from the medium, increasing the pH of the medium. At higher pH, *Synechocystis* cells without the only $Ca^{2+}/H^+$ exchanger probably obtained fewer protons from the medium, and their intracellular pH increased.

**Calcium carbonate precipitation and zeta potential.** To clarify the effect of knocking out *slr1336* on the calcification process in *Synechocystis* 6803, we determined the calcium carbonate precipitation rate. The precipitated calcium was presumed to be absent from the filtered supernatant solution. The rate for the *slr1336*::C.K2 strain was (2.86 ± 0.43) × $10^{-16}$ mol Ca $cell^{-1}$ $h^{-1}$, which was significantly higher than that of the wild type ([1.74 ± 0.28] × $10^{-16}$ mol Ca $cell^{-1}$ $h^{-1}$) under photoautotrophic conditions (*t* test, $P < 0.05$) (Fig. 2A). To determine whether CCM-facilitated photosynthesis affected the $CaCO_3$ precipitation process, we conducted the same measurements under light-activated heterotrophic growth conditions. The calcification rates of both wild-type and *slr1336*::C.K2 mutant cells under light-activated heterotrophic conditions were about 100 times lower than those under photoautotrophic conditions (*t* test, $P < 0.05$) (Fig. 2B). These results suggested that the photosynthetic metabolism process promotes cyanobacterial calcification.

Since the metabolism of cyanobacterial cells can influence their surface potential (35), the zeta potentials of wild-type and *slr1336*::C.K2 cells were measured as a function of pH (Fig. 2C). Both strains had a negatively charged surface over the pH range from 1.27 to 10.00. However, the zeta potential of *slr1336*::C.K2 cells was more negative than that of wild-type cells over a broad range of pH values, suggesting that the mutant cells had a stronger ability to bind $Ca^{2+}$ ions. Cyanobacterial cells can specifically adsorb $Ca^{2+}$ ions onto the cell surface (36). Thus, the lower zeta potential in the *slr1336*::C.K2 cells would reduce the interfacial free energy

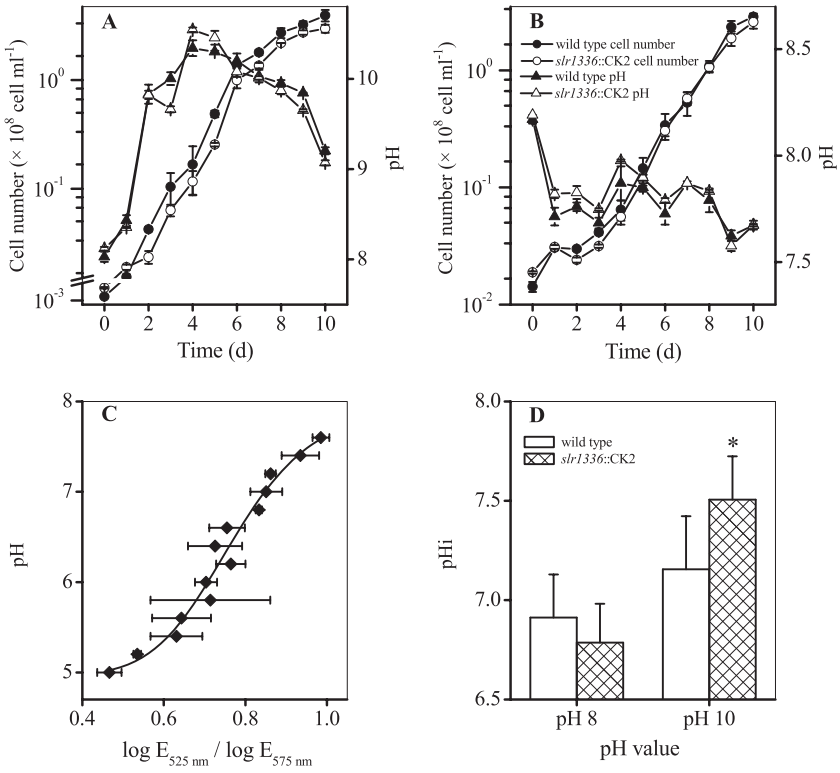


**FIG 1** Cell numbers, growth medium pH, and intracellular pH of *Synechocystis* 6803 wild-type and *slr1336*::C.K2 mutant strains. (A and B) Changes in cell numbers and growth medium pH during growth under autotrophic growth conditions (A) and under light-activated heterotrophic growth conditions (B). The symbol designations in panel B are also used in panel A. (C) *In situ* calibration curve of CF-stained cells measured by flow cytometry. Determined values showed the best fit to a third-order polynomial curve (as shown in the figure). (D) Intracellular pH of *Synechocystis* 6803 wild-type and *slr1336*::C.K2 mutant cells at pH 8.0 or pH 10.0. Conversion from ratio values to pH derived from *in situ* calibration is indicated as the average intracellular pH. Values are means ± SD ($n = 3$ to 6 independent experiments).

of calcite nuclei and accelerate $CaCO_3$ precipitation. The reason why the inactivation of the $Ca^{2+}/H^+$ exchanger resulted in a lower zeta potential in the *slr1336*::C.K2 mutant cells required further research; this is described below.

**Transcriptional analysis of CCM-related genes.** The above results suggested that the $CaCO_3$ precipitation process in *Synechocystis* cells was influenced by CCM-facilitated photosynthesis. The operation of cyanobacterial CCMs can change the pH value of the growth medium (37). Therefore, the expression levels of seven CCM-related genes were compared between wild-type and *slr1336*::C.K2 cells by using quantitative RT-PCR (Fig. 3A). The transcript level of *cmpA* was sharply upregulated in *slr1336*::C.K2

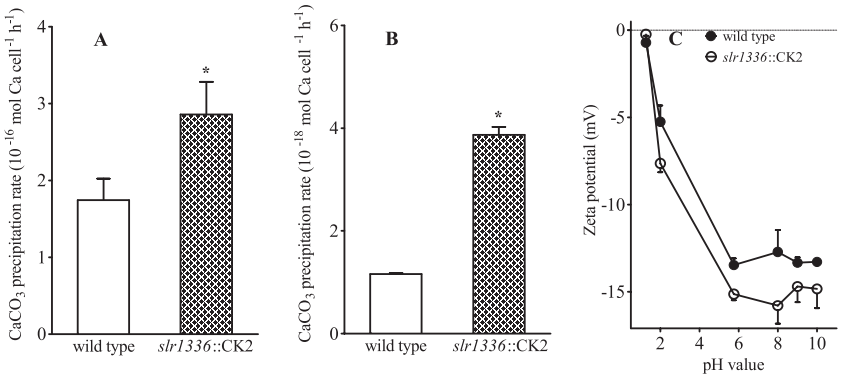


**FIG 2** Calcium precipitation rates and zeta potentials of *Synechocystis* 6803 wild-type and *slr1336*::C.K2 mutant cells. (A) Calcification rate under autotrophic growth conditions. Samples were exposed to 40 μmol photons $m^{-2}$ $s^{-1}$ at 30°C in modified BG11 medium with 3.4 mM $CaCl_2$, 1 mM $KHCO_3$, and 20 mM HEPES-KOH for 3 h. (B) Calcification rate under heterotrophic growth conditions. Cells were cultured in modified BG11 medium as described above and supplemented with 5 mM glucose at 30°C in the dark. (C) Zeta potentials of *Synechocystis* 6803 wild-type and *slr1336*::C.K2 mutant cells in 0.1 M $NaNO_3$ as a function of pH value. Asterisks indicate significant differences between the wild-type and *slr1336*::C.K2 strains (*t* test, $P < 0.05$). Values are means ± SD ($n = 3$ to 4 independent experiments).

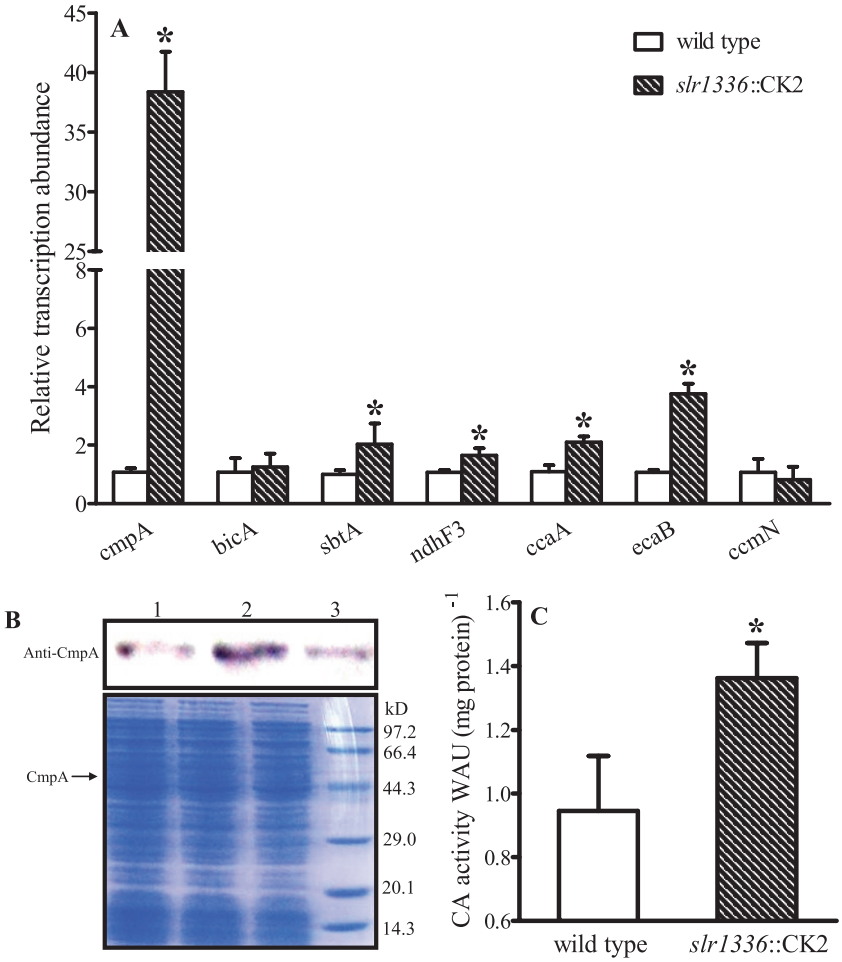


**FIG 3** Effects of disruption of the *slr1336* gene on CCMs. (A) Relative transcript abundance of several CCM-related genes in *slr1336*::C.K2 mutant cells compared with that in *Synechocystis* 6803 wild-type cells. Values are means ± SD ($n = 4$ replicate measurements). (B) Protein levels of CmpA in *Synechocystis* 6803 wild-type, *slr1336*::C.K2 mutant, and complemented (*slr1336*::C.K2+psbAII $_{slr1336}$) cells grown in BG11 medium. Lane 1, wild type; lane 2, *slr1336*::C.K2; lane 3, *slr1336*::C.K2+psbAII $_{slr1336}$. Total protein (10 μg) from each sample was separated by SDS-PAGE (lower panel) and subjected to Western blotting (upper panel). (C) Total CA activity in crude extracts of *Synechocystis* 6803 wild-type and *slr1336*::C.K2 mutant cells. Values are means ± SD ($n = 3$ independent experiments).

mutant cells, to a level more than 30 times that in the wild type. *cmpA* encodes a subunit of the BCT1 $HCO_3^-$ transporter, which has a $Ca^{2+}$-binding site (38). For the $Na^+$-dependent $HCO_3^-$ transporters, *sbtA* was upregulated in *slr1336*::C.K2 cells to a level 2-fold that in the wild type, while similar levels of *bicA* transcripts were detected in the mutant and wild type. *ndhF3*, which encodes a low-$C_i$-induced $CO_2$ transport system, was upregulated about 1.5-fold in *slr1336*::C.K2 relative to wild-type cells. The genes encoding carboxysome CA (*ccaA*) and a possible periplasmic CA (*ecaB*) showed similar transcription patterns; their transcripts were upregulated approximately 2- and 3-fold, respectively, in *slr1336*::C.K2 relative to wild-type cells. From these results, we concluded that the inactivation of the $Ca^{2+}/H^+$ exchanger (Slr1336) stimulated the expression levels of CCM-related genes, especially *cmpA*, which encodes the BCT1 $HCO_3^-$ transporter. Interestingly, the upregulation of these CCM-related genes was consistent with the increased calcification rate in *slr1336*::C.K2 (Fig. 2).

**Western blot analysis of CmpA protein and total CA activity analysis.** To determine whether the upregulation of *cmpA* transcription led to an increase at the protein level, Western blot analysis was performed using a CmpA antibody (Fig. 3B). When equal amounts of total proteins from wild-type and *slr1336*::C.K2 cells were analyzed, the amount of CmpA was higher in *slr1336*::C.K2 than in wild-type cells. We also constructed a *slr1336*::C.K2-complemented strain (*slr1336*::C.K2+psbAII $_{slr1336}$) by expressing the *slr1336* gene in the *slr1336*::C.K2 mutant with a PsbAII expression vector (23). The complemented strain further confirmed that the phenotypes of the mutant were caused by the inactivation of *slr1336*, and they excluded a second site mutation. When equal amounts of total proteins were analyzed, there was less CmpA protein in complemented cells than in *slr1336*::C.K2 cells, but the level was similar to that in wild-type cells.

Since the transcriptional analysis indicated that CA-encoding genes were upregulated in the *slr1336*::C.K2 mutant, CA activity was measured to examine whether the upregulated transcript levels of *ccaA* and *ecaB* enhanced the enzymatic activity of *slr1336*::C.K2 cells (Fig. 3C). The total CA activity of *slr1336*::C.K2 was 1.36 ± 0.11 WAU mg of protein$^{-1}$, which was significantly higher than that of the wild type (0.94 ± 0.17 WAU mg

**TABLE 1** $C_i$ fluxes of *Synechocystis* 6803 wild type, *slr1336*::C.K2, and the *slr1336/cmpA* double mutant[a]

| Strain | $C_i$ flux (μmol $C_i$ mg Chl $a^{-1}$ $h^{-1}$) | | | |
|---|---|---|---|---|
| | Net $HCO_3^-$ uptake | Net $CO_2$ uptake | Influx of $CO_2$ | Leakage of $CO_2$ |
| Wild type | 155.4 ± 32.4 a | 28.2 ± 17.4 a | 52.8 ± 8.4 a | 24.6 ± 10.8 ab |
| *slr1336*::C.K2 | 227.4 ± 5.4 b | 26.4 ± 7.2 a | 62.4 ± 18.6 a | 36.6 ± 18.0 a |
| *slr1336/cmpA* | 129.6 ± 24.0 a | 12.0 ± 5.4 a | 20.4 ± 3.0 b | 8.4 ± 4.8 b |

[a] Cells were resuspended in fresh modified BG11 medium, and $CO_2$ and $O_2$ concentrations in cell suspensions were monitored simultaneously with a MIMS apparatus during dark/light/dark transitions after addition of 100 μM $KHCO_3$ at pH 8.0, 30°C, and 500 μmol photons $m^{-2}$ $s^{-1}$. Values in the same column followed by different lowercase letters are significantly different (Tukey multiple comparison, $P < 0.05$). Values are means ± SD ($n = 4$ independent experiments).

of protein$^{-1}$; *t* test, $P < 0.05$). These findings were consistent with the qPCR results shown in Fig. 3A.

**$C_i$ flux and photosynthetic $O_2$ evolution.** The $O_2$ and $CO_2$ concentrations of the *Synechocystis* 6803 wild type, *slr1336*::C.K2, and *slr1336/cmpA* double mutant were measured by using a membrane inlet mass spectrometer at pH 8.0 according to the methods described by Badger et al. (31). The net $HCO_3^-$ uptake rate of *slr1336*::C.K2 was significantly higher than that of the wild type (Tukey multiple comparison, $P < 0.05$) (Table 1). The net $CO_2$ uptake, $CO_2$ leakage, and influx rates showed no significant differences between the wild type and *slr1336*::C.K2 (Tukey multiple comparison, $P > 0.05$). For the double mutant of *slr1336* and *cmpA*, the net $HCO_3^-$ uptake rate was close to that of the wild type (Tukey multiple comparison, $P > 0.05$), but it was significantly less than that of *slr1336*::C.K2 (Tukey multiple comparison, $P < 0.05$).

Next, we analyzed the photosynthetic contributions of different $C_i$ transport systems by determining oxygen evolution rates after adding different $C_i$ uptake inhibitors at pH 8.0 (Table 2). When 25 mM LiCl plus 300 μM EZ was added, only the BCT1 $Na^+$-independent $HCO_3^-$ transporter operated. Under these conditions, the photosynthetic rate of *slr1336*::C.K2 cells was 115.2 ± 27.6 μmol $O_2$ mg Chl $a^{-1}$ $h^{-1}$, which was significantly higher than that of wild-type cells (69.0 ± 15.0 μmol $O_2$ mg Chl $a^{-1}$ $h^{-1}$; *t* test, $P < 0.05$). This suggested that photosynthetic activity supported by BCT1 $HCO_3^-$ transporter uptake systems is induced in *slr1336*::C.K2 cells. This finding was consistent with the results of qRT-PCR and Western blot analyses (Fig. 3A and B). The photosynthetic activity supported either by $CO_2$ uptake systems or by $Na^+$-dependent $HCO_3^-$ transporters (SbtA and BicA) showed no significant difference between the mutant and wild type (*t* test, $P > 0.05$).

## DISCUSSION

According to the model proposed by Riding (17), cyanobacterial calcification is promoted by $CO_2$-concentrating mechanisms that developed to accommodate photosynthetic carbon limitation. The model states that CCMs actively import DIC into the cell for photosynthetic carbon fixation, meanwhile liberating $OH^-$ ions out of the cell. This raises the external pH and thus stimulates $CaCO_3$ precipitation at high ambient carbonate saturation (17). The results reported here support this model. *Synechocystis* 6803 can utilize glucose as a carbon source and perform light-activated heterotrophic growth (21). Thus, it is a good model organism to investigate the effects of photosynthesis on cyanobacterial calcification. Our data showed that when cultured in medium with a high $Ca^{2+}$ concentration (3.4 mM $CaCl_2$), the calcification rate of cells grown under photoautotrophic conditions was 100 times higher than that in cells grown under light-activated heterotrophic conditions (Fig. 2). According to the amount of Chl *a* per cell, it can reach up to 3.0% and 4.5% of the maximum photosynthetic rate, respectively, for wild-type and *slr1336*::C.K2 cells grown under photoautotrophic condition (measured at 40 μmol photons $m^{-2}$ $s^{-1}$) (Fig. 2; Table 2). In spite of certain physiological differences between the two strains, the dramatic increase in the calcification rate under photoautotrophic conditions indicated the significant roles of photosynthesis in the process of cyanobacterial calcification. Under heterotrophic conditions, cyanobacteria cannot drive photosynthetic $C_i$ transport and $CO_2$ assimilation via the Calvin cycle. Consequently, the major metabolic pathway switches to the oxidative pentose phosphate pathway (OPPP) and the tricarboxylic acid cycle (39, 40), and therefore calcification barely occurs outside the cells.

When the only $Ca^{2+}/H^+$ exchanger was knocked out in *Synechocystis* cells, fewer $Ca^{2+}$ ions were transported to the periplasmic space and fewer protons were transported into the cytoplasm (19). This variation in the $Ca^{2+}$ concentration in the periplasm probably caused a series of expression changes of genes regulated by the $Ca^{2+}$ concentration, such as *cmpA*. In *Synechococcus* sp. strain PCC 7942, the *cmpABCD* operon plays essential roles in $HCO_3^-$ transport (41, 42). In *Synechocystis* 6803, the key roles of

**TABLE 2** Photosynthetic rates of *Synechocystis* 6803 wild-type and *slr1336*::C.K2 mutant cells supported by different $C_i$ transporters[a]

| Treatment (data derivation no.) | Operation of $C_i$ transport system(s) | Photosynthetic rate (μmol $O_2$ mg Chl $a^{-1}$ $h^{-1}$) | |
|---|---|---|---|
| | | Wild type | *slr1336*::C.K2 |
| 25 mM NaCl (1) | BCT1, SbtA, and BicA $HCO_3^-$ transporters; $CO_2$ transport systems | 201.0 ± 25.2 | 223.8 ± 33.6 |
| 25 mM NaCl + 300 μM EZ (2) | BCT1, SbtA, and BicA $HCO_3^-$ transporters | 164.4 ± 28.8 | 198.6 ± 37.8 |
| 25 mM LiCl + 300 μM EZ (3) | BCT1 $HCO_3^-$ transporter | 69.0 ± 15.0 | 115.2 ± 27.6* |
| Rates for derivation 2 − derivation 3 | SbtA and BicA $HCO_3^-$ transporters | 95.4 ± 23.4 | 83.4 ± 36.0 |
| Rates for derivation 1 − derivation 2 | $CO_2$ transport systems | 36.6 ± 12.0 | 25.2 ± 15.0 |

[a] Samples were washed and resuspended in $NO_3^-$-free, $Na^+$-free, and $C_i$-free BG11 medium buffered with 20 mM HEPES-KOH (pH 8.0). Then, 1 mM $KHCO_3$ was added after $C_i$ depletion at 150 μmol photons $m^{-2}$ $s^{-1}$, and the photosynthetic rate was measured at 650 μmol photons $m^{-2}$ $s^{-1}$ and 30°C under three treatments (25 mM NaCl, 25 mM NaCl plus 300 μM EZ, 25 mM LiCl plus 300 μM EZ). $CO_2$ transport systems were inhibited by addition of 300 μM EZ; $Na^+$-dependent $HCO_3^-$ transporters (SbtA and BicA) were inhibited by addition of 25 mM LiCl and removal of $Na^+$. The asterisk indicates a significant difference between *slr1336*::C.K2 and the wild-type strain (*t* test, $P < 0.05$). Values are means ± SD (n = 6 independent experiments).

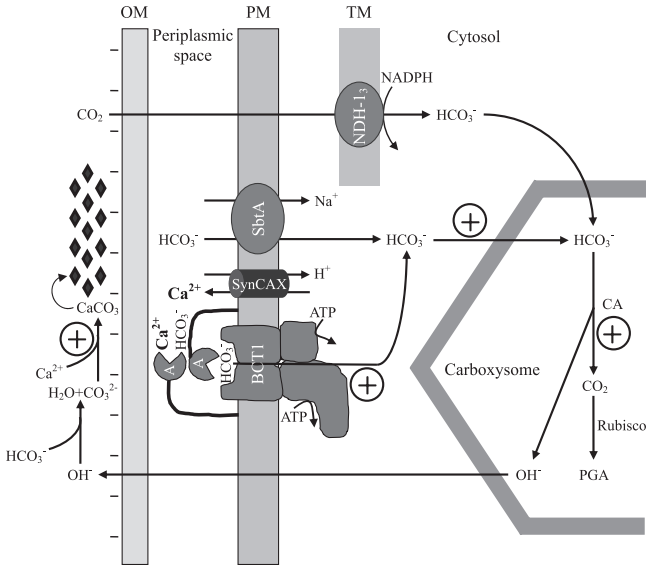


**FIG 4** Scheme showing cyanobacterial calcification promoted by inactivation of $Ca^{2+}/H^+$ exchanger. CCMs function to transport $C_i$ into the cytosol, where DIC accumulates as $HCO_3^-$. The pool of $HCO_3^-$ converts to $CO_2$ for photosynthetic carbon fixation in the carboxysome and liberates $OH^-$ ions from the cell, raising the external pH. Inactivation of the $Ca^{2+}/H^+$ exchanger decreases the zeta potential, induces the BCT1 $HCO_3^-$ transporter, increases CA activity, and thus increases the pH in the microenvironment around the cell. This can stimulate $CaCO_3$ precipitation by increasing ambient carbonate saturation. The + symbol indicates upregulated steps demonstrated in the present study. A, CmpA; OM, outer membrane; PGA, glycerate-3-phosphate; PM, plasma membrane; Rubisco, ribulose bisphosphate carboxylase-oxygenase; TM, thylakoid membrane.

the CmpA protein or the BCT1 $HCO_3^-$ transporter still need to be elucidated, since the inactivation of the *cmp* operon in an *ndhB* mutant of *Synechocystis* 6803 did not change its growth characteristics at pH 9.0 (DIC was mainly supplied by $HCO_3^-$) (43). Interestingly, the structure of CmpA in *Synechocystis* 6803 has already been reported; the *Synechocystis* CmpA protein is anchored at the plasma membrane, and its $Ca^{2+}$-binding site is exposed at the periplasmic side. The binding of bicarbonate to CmpA is accompanied by a $Ca^{2+}$ ion, which probably acts a cofactor in the bicarbonate transport activity of CmpA (38). Although limitation in the methodology did not allow measurement of the $Ca^{2+}$ concentration in the periplasm in this study, we suggest that a short-term decrease in the $Ca^{2+}$ concentration in the periplasmic space could be the signal to induce expression of *cmpA*. This hypothesis is also consistent with the phylogenetic distribution of the *cmp* operon or BCT1 among different cyanobacterial species. BCT1 is generally present in freshwater cyanobacterial species but not in marine ones, except for *Synechococcus* WH5701 (16, 44); it is interesting that the concentration of calcium is much lower in freshwater than in seawater (6). The relatively lower $Ca^{2+}$ concentration in the periplasmic space in the *slr1336*::C.K2 mutant might be the main reason for upregulation of the *cmpA* gene. This hypothesis was supported by our results, including the increased protein level of CmpA as determined by Western blot analysis (Fig. 3), the increase of net $HCO_3^-$ uptake as determined by the MIMS assay (Table 1), and the increased photosynthetic rate supported by the BCT1 transporter (Table 2). The model in Fig. 4 shows the putative mechanism of cyanobacterial calcification promoted by the inactivation of the $Ca^{2+}/H^+$ exchanger.

In addition to the change in $Ca^{2+}$ concentration, the intracellular pH and zeta potential of the *slr1336*::C.K2 mutant were also affected by the inactivation of the $Ca^{2+}/H^+$ exchanger (Syn CAX). When the pH of the growth medium was 10, the intracellular pH was higher in *slr1336*::C.K2 mutant cells than in wild-type cells (Fig. 1). This result is consistent with the conclusion of Waditee et al. (19), who reported that Slr1336 catalyzes the $Ca^{2+}/H^+$ exchange reaction at alkaline pH with a stoichiometry of $H^+$:$Ca^{2+}$ higher than 2. The increase in intracellular pH would result in a relatively lower $CO_2/HCO_3^-$ ratio within the cell, which could result in upregulation of the low-$C_i$-induced $CO_2$ transport system encoded by *ndhF3* and of CA-encoding genes (Fig. 3). The results of several independent experiments in this study showed that the zeta potentials of both wild-type and *slr1336*::C.K2 cells were negative over a broad pH range (Fig. 2). These findings were consistent with previously reported results that showed that most microorganisms exhibit a negative zeta potential at pH levels of >2.0 (35). Evidently, the *slr1336*::C.K2 mutant cells exhibited a lower zeta potential than wild-type cells, and thus, they may bind cations such as $Ca^{2+}$ more easily. This might contribute greatly to the higher calcification rate in *slr1336*::C.K2 cells.

In conclusion, the mutation of the $Ca^{2+}/H^+$ exchanger (Slr1336) in *Synechocystis* 6803 cells activated CCM-related genes and increased the activities of $C_i$ transport systems, especially that of the BCT1 transporter. As a result, the *slr1336*::C.K2 mutant cells showed higher $HCO_3^-$ uptake than wild-type cells and increased the pH of the microenvironment around the cells to promote the calcification process. The lower zeta potential of mutant cells indicated a greater ability to bind calcium ions, thus facilitating $CaCO_3$ precipitation (Fig. 4).

## ACKNOWLEDGMENTS

This study was funded by the National Natural Science Foundation of China (grant numbers 31100184 and 31170309).

## REFERENCES

1. **Arp G, Reimer A, Reitner J.** 2001. Photosynthesis-induced biofilm calcification and calcium concentrations in Phanerozoic oceans. Science **292:**1701–1704.
2. **Dittrich M, Kurz P, Wehrli B.** 2004. The role of autotrophic picocyanobacteria in calcite precipitation in an oligotrophic lake. Geomicrobiol. J. **21:**45–53.
3. **Riding R.** 2006. Cyanobacterial calcification, carbon dioxide concentrating mechanisms, and Proterozoic-Cambrian changes in atmospheric composition. Geobiology **4:**299–316.
4. **Thompson JB, Schultze-Lam S, Beveridge TJ, Des Marais DJ.** 1997. Whiting events: biogenic origin due to the photosynthetic activity of cyanobacterial picoplankton. Limnol. Oceanogr. **42:**133–141.
5. **Altermann W, Kazmierczak J, Oren A, Wright DT.** 2006. Cyanobacterial calcification and its rock-building potential during 3.5 billion years of Earth history. Geobiology **4:**147–166.
6. **Dittrich M, Obst M.** 2004. Are picoplankton responsible for calcite precipitation in lakes? Ambio **33:**559–564.
7. **Jansson C, Northen T.** 2010. Calcifying cyanobacteria—the potential of biomineralization for carbon capture and storage. Curr. Opin. Biotechnol. **21:**365–371.
8. **Thompson JB, Ferris FG.** 1990. Cyanobacterial precipitation of gypsum, calcite, and magnesite from natural alkaline lake water. Geology **18:**995–998.
9. **Couradeau E, Benzerara K, Gérard E, Moreira D, Bernard S, Brown GE, López-García P.** 2012. An early-branching microbialite cyanobacterium forms intracellular carbonates. Science **336:**459–462.
10. **Merz M.** 1992. The biology of carbonate precipitation by cyanobacteria. Facies **26:**81–101.
11. **Lee BD, Apel WA, Walton MR.** 2006. Calcium carbonate formation by

*Synechococcus* sp. strain PCC 8806 and *Synechococcus* sp. strain PCC 8807. Bioresour. Technol. **97:**2427–2434.
12. **Homa ES, Chapra SC.** 2011. Modeling the impacts of calcite precipitation on the epilimnion of an ultraoligotrophic, hard-water lake. Ecol. Model. **222:**76–90.
13. **Kawaguchi T, Decho AW.** 2002. A laboratory investigation of cyanobacterial extracellular polymeric secretions (EPS) in influencing $CaCO_3$ polymorphism. J. Cryst. Growth **240:**230–235.
14. **Giordano M, Beardall J, Raven JA.** 2005. $CO_2$ concentrating mechanisms in algae: mechanisms, environmental modulation, and evolution. Annu. Rev. Plant Biol. **56:**99–131.
15. **Kaplan A, Reinhold L.** 1999. $CO_2$ concentrating mechanisms in photosynthetic microorganisms. Annu. Rev. Plant Biol. **50:**539–570.
16. **Price GD, Badger MR, Woodger FJ, Long BM.** 2008. Advances in understanding the cyanobacterial $CO_2$-concentrating-mechanism (CCM): functional components, Ci transporters, diversity, genetic regulation and prospects for engineering into plants. J. Exp. Bot. **59:**1441–1461.
17. **Riding R.** 2009. An atmospheric stimulus for cyanobacterial-bioinduced calcification ca. 350 million years ago? Palaios **24:**685–696.
18. **Obst M, Wehrli B, Dittrich M.** 2009. $CaCO_3$ nucleation by cyanobacteria: laboratory evidence for a passive, surface-induced mechanism. Geobiology **7:**324–347.
19. **Waditee R, Hossain GS, Tanaka Y, Nakamura T, Shikata M, Takano J, Takabe T, Takabe T.** 2004. Isolation and functional characterization of $Ca^{2+}/H^+$ antiporters from cyanobacteria. J. Biol. Chem. **279:**4330–4338.
20. **Stanier R, Kunisawa R, Mandel M, Cohen-Bazire G.** 1971. Purification and properties of unicellular blue-green algae (order Chroococcales). Bacteriol. Rev. **35:**171–205.
21. **Anderson SL, McIntosh L.** 1991. Light-activated heterotrophic growth of the cyanobacterium *Synechocystis* sp. strain PCC 6803: a blue-light-requiring process. J. Bacteriol. **173:**2761–2767.
22. **Marie D, Simon N, Vaulot D.** 2005. Phytoplankton cell counting by flow cytometry, p 254–278. *In* Andersen RA (ed), Algal culturing techniques. Elsevier Academic Press, Burlington, MA.
23. **Jiang HB, Lou WJ, Du HY, Price NM, Qiu BS.** 2012. Sll1263, a unique cation diffusion facilitator protein that promotes iron uptake in the cyanobacterium *Synechocystis* sp. strain PCC 6803. Plant Cell Physiol. **53:**1404–1417.
24. **Williams JGK.** 1988. Construction of specific mutations in photosystem II photosynthetic reaction center by genetic engineering methods in *Synechocystis* 6803, p 766–778. *In* Colowick SP, Kaplan NO, Packer L, Glazer AN (ed), Methods in enzymology. Academic Press, New York, NY.
25. **Pybus J, Feldman FJ, Bowers GN.** 1970. Measurement of total calcium in serum by atomic absorption spectrophotometry, with use of a strontium internalreference. Clin. Chem. **16:**998–1007.
26. **Dittrich M, Sibler S.** 2005. Cell surface groups of two picocyanobacteria strains studied by zeta potential investigations, potentiometric titration, and infrared spectroscopy. J. Colloid. Interf. Sci. **286:**487–495.
27. **Weigert C, Steffler F, Kurz T, Shellhammer TH, Methner FJ.** 2009. Application of a short intracellular pH method to flow cytometry for determining *Saccharomyces cerevisiae* vitality. Appl. Environ. Microbiol. **75:**5615–5620.
28. **Livak KJ, Schmittgen TD.** 2001. Analysis of relative gene expression data using real-time quantitative PCR and the $2^{-\Delta\Delta CT}$ method. Methods **25:**402–408.
29. **Wilbur KM, Anderson NG.** 1948. Electrometric and colorimetric determination of carbonic anhydrase. J. Biol. Chem. **176:**147–154.
30. **Song YF, Qiu BS.** 2007. The $CO_2$-concentrating mechanism in the bloom-forming cyanobacterium *Microcystis aeruginosa* (Cyanophyceae) and effects of UVB radiation on its operation. J. Phycol. **43:**957–964.
31. **Badger MR, Palmqvisl K, Yu JW.** 1994. Measurement of $CO_2$ and $HCO_3^-$ fluxes in cyanobacteria and microalgae during steady-state photosynthesis. Physiol. Plant. **90:**529–536.
32. **Espie GS, Kandasamy RA.** 1994. Monensin inhibition of $Na^+$-dependent $HCO_3^-$ transport distinguishes it from $Na^+$-independent $HCO_3^-$ transport and provides evidence for $Na^+/HCO_3^-$ symport in the cyanobacterium *Synechococcus* UTEX 625. Plant Physiol. **104:**1419–1428.
33. **Miller AG, Espie GS, Canvin DT.** 1990. Physiological aspects of $CO_2$ and $HCO_3^-$ transport by cyanobacteria: a review. Can. J. Bot. **68:**1291–1302.
34. **Price GD, Badger MR.** 1989. Ethoxyzolamide inhibition of $CO_2$ uptake in the cyanobacterium *Synechococcus* PCC7942 without apparent inhibition of internal carbonic anhydrase activity. Plant Physiol. **89:**37–43.
35. **Martinez RE, Pokrovsky OS, Schott J, Oelkers EH.** 2008. Surface charge and zeta-potential of metabolically active and dead cyanobacteria. J. Colloid. Interf. Sci. **323:**317–325.
36. **Obst M, Dittrich M, Kuehn H.** 2006. Calcium adsorption and changes of the surface microtopography of cyanobacteria studied by AFM, CFM, and TEM with respect to biogenic calcite nucleation. Geochem. Geophys. Geosyst. **7:**Q06011.
37. **Ogawa T, Kaplan A.** 1987. The stoichiometry between $CO_2$ and $H^+$ fluxes involved in the transport of inorganic carbon in cyanobacteria. Plant Physiol. **83:**888–891.
38. **Koropatkin NM, Koppenaal DW, Pakrasi HB, Smith TJ.** 2007. The structure of a cyanobacterial bicarbonate transport protein, CmpA. J. Biol. Chem. **282:**2606–2614.
39. **Knowles VL, Plaxton WC.** 2003. From genome to enzyme: analysis of key glycolytic and oxidative pentose-phosphate pathway enzymes in the cyanobacterium *Synechocystis* sp. PCC 6803. Plant Cell Physiol. **44:**758–763.
40. **Zhang S, Bryant DA.** 2011. The tricarboxylic acid cycle in cyanobacteria. Science **334:**1551–1553.
41. **Maeda S, Price GD, Badger MR, Enomoto C, Omata T.** 2000. Bicarbonate binding activity of the CmpA protein of the cyanobacterium *Synechococcus* sp. strain PCC 7942 involved in active transport of bicarbonate. J. Biol. Chem. **275:**20551–20555.
42. **Omata T, Price GD, Badger MR, Okamura M, Gohta S, Ogawa T.** 1999. Identification of an ATP-binding cassette transporter involved in bicarbonate uptake in the cyanobacterium *Synechococcus* sp. strain PCC 7942. Proc. Natl. Acad. Sci. U. S. A. **96:**13571–13576.
43. **Shibata M, Katoh H, Sonoda M, Ohkawa H, Shimoyama M, Fukuzawa H, Kaplan A, Ogawa T.** 2002. Genes essential to sodium-dependent bicarbonate transport in cyanobacteria: function and phylogenetic analysis. J. Biol. Chem. **277:**18658–18664.
44. **Badger MR, Price GD, Long BM, Woodger FJ.** 2006. The environmental plasticity and ecological genomics of the cyanobacterial $CO_2$ concentrating mechanism. J. Exp. Bot. **57:**249–265.